Appl. Phys. B 89, 385–394 (2007)
DOI: 10.1007/s00340-007-2804-6

Applied Physics B
Lasers and Optics

ANIL KUMAR✉
R. RAJESH
GAURAV SINGHAL
R.K. TYAGI

Analysis of various optical pumping schemes for liquid oxygen lasers

Laser Science and Technology Center, Metcalfe House, Delhi 110054, India

Received: 16 June 2007/Accepted: 12 September 2007
Published online: 23 October 2007 •

ABSTRACT Singlet oxygen generated by optical pumping in liquid oxygen/air medium has recently been reported as a potential gain medium for high power lasers at 1580 nm, by USA's defense agency DARPA. However, the details with reference to the underlying physics of this laser and the potential pumping techniques for achieving lasing are still unclear. The present paper investigates numerically the population kinetics of both upper and lower lasing levels viz. O_2 $(^1\Delta_g)_{v=0}$ and $O_2(^3\Sigma_g)_{v=1}$ states in liquid oxygen and discusses the criticality involved in obtaining lasing with this medium. Isotopic liquid oxygen and liquid air medium where improved conditions for lasing are anticipated, as compared to that in natural liquid oxygen, have also been considered in the present study. The studies have been carried out for optical pumping by both continuous and pulsed mode lasers at 1064 nm and 634 nm wavelengths. The temporal variation of small signal gain in each case has been investigated along with limitations of the same from point of view of lasing. The available and extractable power from all three medium for an optimum pumping case has also been discussed. The studies reveal that liquid air has high potential for very high power lasers as compared to both natural and isotopic liquid oxygen.

PACS 31.15.ag

1 Introduction

The search for an ideal lasing species with energy levels having appropriate meta-stable lifetime has been a quest for researchers from the day of laser invention. High power continuous wave lasers (multi-kilowatt) have wide applications in both civil as well as defense areas. Even though megawatt class continuous wave lasers: hydrogen/deuterium fluoride lasers (HF/DF), chemical oxygen iodine lasers (COIL), CO_2 gas dynamic laser (GDL), etc. are available at present, their applications to a large extent have been limited by issues pertaining to compactness. Further, handling of hazardous chemicals, operational easiness and readiness time are the other practical issues related to the above high power lasers. These limit their applications and make it imperative to search for new lasing mediums. Therefore, the search for an extremely low specific weight (weight per unit power output) and eco-friendly laser still remains a front line area of interest among laser researchers. The first electronically excited level of oxygen molecules, the singlet delta oxygen $O_2(^1\Delta_g)$, is one such species which fulfills the desired properties of a near ideal lasing medium. Various methods such as optical, electrical and chemical have been utilized for the generation of these singlet delta oxygen molecules. Among these, the most efficient method is chemical one and generated singlet delta oxygen has been efficiently used as the pumping medium in COIL [1]. However, all these singlet oxygen generation techniques have failed to yield a stimulated emission condition, in either of its strong emission lines at 1268 nm or 1580 nm. Until very recently, the research in singlet oxygen generation had primarily advanced from the viewpoint of its application as a pumping source in COIL rather than as a lasing medium.

The exploration of liquid oxygen as a lasing medium started in mid-1970s [2]. But success in terms of lasing was reported only recently, in 2005, by USA's DARPA organization [3]. The physics and techniques of this laser have not been published. Optical excitation of the gas phase oxygen molecules is extremely inefficient due to its very low absorption coefficient. In the liquid phase (97 K) the oxygen molecules exist in 'pair' form, which increases their absorption coefficient many folds for its various characteristic lines [4]. This makes optical pumping in liquid oxygen efficient and hence opens up the possibility of very high density production of meta-stable oxygen molecules. During such optical pumping, successive electronic to vibrational transfer (E–V transfer) and vibrational to vibrational (V–V) relaxation of the higher levels is found to occur. The $O_2(^3\Sigma_g)_{v=1}$ is another meta-stable level which has a long lifetime of ~ 2.5 ms in case of pure natural liquid oxygen. This leads to accumulation at the longer living first vibrational level of the ground molecules, $O_2(^3\Sigma_g)_{v=1}$. Hence, under steady state condition, liquid oxygen medium gives way for a three-level laser configuration with emission between $O_2(^1\Delta_g)_{v=0}$ and $O_2(^3\Sigma_g)_{v=1}$ levels at 1580 nm.

In this paper, detailed investigation on the population kinetics of the upper $[O_2(^1\Delta_g)_{v=0}]$ and lower $[O_2(^3\Sigma_g)_{v=1}]$ lasing levels have been presented. The procedure employed considers various decay processes along with setting up the corresponding rate equations utilizing the observed rate con-

✉ Fax: +91 11 2381 1319, E-mail: anil4k@gmail.com

stants by various experimental works. Continuous as well as pulsed pumping options employing sources having 1064 nm and 634 nm wavelengths with various power densities are considered. Further, the analysis has been conducted for three different oxygen rich cryo-mediums considering their corresponding kinetics to arrive at the best possible option. The temporal evolutions of the small signal gain in each case and power extraction analysis for the best possible cases are also discussed.

2 Laser chemical kinetics and physics

The absorption and emission lines of liquid oxygen have been explained theoretically and experimentally by many researchers [2, 4, 5]. Detailed study on the absorption lines of oxygen in the liquid phase and gas at very high densities is reported by Zhdanov et al. [4]. The above studies clearly indicate that the absorption cross section is improved many folds for almost all lines in liquid oxygen as compared to that in gaseous oxygen, which confirms the existence of pair molecules in liquid phase. Considering the existence of pair molecules in liquid oxygen, major energy level scheme for co-operative emissions and absorptions in liquid oxygen is shown in Fig. 1. The major absorption lines of liquid oxygen are 470 nm, 581 nm, 634 nm, 764 nm, 1064 nm and 1268 nm with relative absorption coefficients being 2.4, 7.1, 5.1, 1.0, 5.4 and 6.8 respectively [4]. On the other hand the major emission lines are the following: 581 nm, 634 nm, 703 nm, 1268 nm and 1580 nm, having relative emission intensities [2, 6] as 0.03, 1.0, 1.0, 3.0×10^4 and 1.0×10^4 respectively. This indicates that the emissions at 1268 nm and 1580 nm form the maximum probable emission lines in the liquid oxygen medium from viewpoint of lasing. The strongest emission line, 1268 nm, is also a strong absorption line in liquid oxygen limiting its chance of being a lasing line. Therefore, 1580 nm emission is expected to be the prominent lasing line as it has almost zero absorption at this wavelength.

In liquid oxygen, the lifetime of the higher electronic state ($O_2\,^1\Sigma$), the vibrational levels of the first electronic level, $(O_2\,^1\Delta)_{v=1-3}$, and the higher vibrational levels of the ground state molecules, $(O_2\,^3\Sigma)_{v>1}$, are very low and hence quench and relax very rapidly. This is well supported by various experimental studies [7, 8], where no spontaneous anti-Stokes Raman scattering lines from any vibrational levels $(O_2\,^3\Sigma)_{v>1}$ were observed. The only line observed was for $O_2{}^3\Sigma_{v=1}$ level. Therefore, under steady state condition, simply a three level scheme in liquid oxygen can be considered as shown in Fig. 2.

Correspondingly, the stimulated emission process can be expressed as:

$$O_2\left(^1\Delta_g\right)_{v=0} + 1h\upsilon(1580\,\text{nm}) \rightarrow \text{O}_2\left(^3\Sigma_g\right)_{v=1} + 2h\upsilon\,. \qquad (1)$$

Considering the strong absorption lines in liquid oxygen, sources with wavelengths 581 nm, 634 nm, 1060 nm and 1268 nm sources can be used for the excitation to the first excited electronic level of oxygen. Hence, the pumping to the upper lasing level can be carried out with any of these following photon excitation [5, 9] processes:

$$2\text{O}_2\,(\,^3\Sigma_g)_{v=0} + h\upsilon(581\,\text{nm}) \rightarrow \text{O}_2\,(\,^1\Delta_g)_{v=0} + \text{O}_2\,(\,^1\Delta_g)_{v=1}\,, \qquad (2)$$

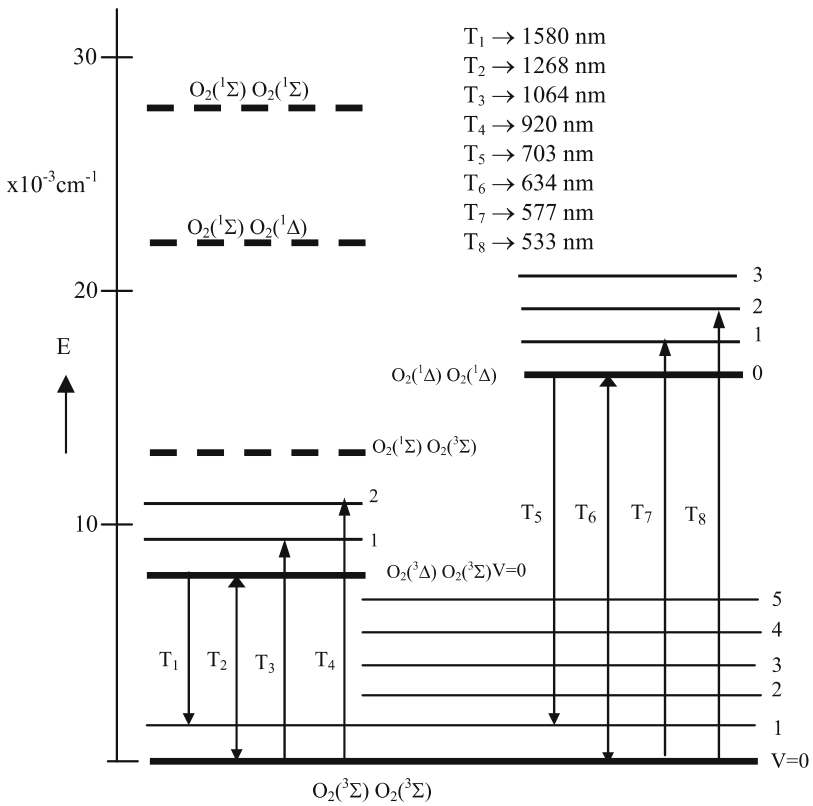

FIGURE 1 Energy level scheme in liquid oxygen

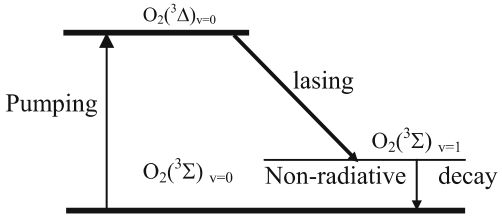

FIGURE 2 A possible three level lasing scheme in liquid oxygen

$$2O_2\,(^3\Sigma_g)_{v=0} + h\upsilon(1064\,\text{nm}) \rightarrow O_2\,(^1\Delta_g)_{v=0} + O_2\,(^3\Sigma_g)_{v=1}\,, \quad (3)$$

$$2O_2\,(^3\Sigma_g)_{v=0} + h\upsilon(1064\,\text{nm}) \rightarrow O_2\,(^1\Delta_g)_{v=1} + O_2\,(^3\Sigma_g)_{v=0}\,, \quad (4)$$

$$2O_2\,(^3\Sigma_g)_{v=0} + h\upsilon(634\,\text{nm}) \rightarrow 2O_2\,(^1\Delta_g)_{v=0}\,, \quad (5)$$

$$O_2\,(^3\Sigma_g)_{v=0} + h\upsilon(1268\,\text{nm}) \rightarrow O_2\,(^1\Delta_g)_{v=0}\,. \quad (6)$$

In processes (2) and (4), even though one $(^1\Delta_g)_{v=1}$ level is generated for each photon, it will rapidly quench to the needed $(^1\Delta_g)_{v=0}$ level through the process,

$$O_2\,(^1\Delta_g)_{v=1} + O_2\left(^3\Sigma_g\right)_{v=0} \rightarrow O_2\,(^1\Delta_g)_{v=0} + O_2\,(^3\Sigma_g)_{v=1}\,,$$
$$k = 3.4\times10^{-14}(T_0/T)^{-\frac{1}{2}}\,\text{cm}^3\text{mol}^{-1}\text{s}^{-1}\,. \quad (7)$$

However, it will be disadvantageous for lasing, since it simultaneously populates the lower lasing level, i.e., one $O_2(^3\Sigma)_{v=1}$ molecule will also be generated along with the desired $O_2(^1\Delta_g)_{v=0}$. Therefore, overall optical pumping in liquid oxygen is a complex process, and hence the numerical studies are essential to determine the population in the corresponding energy levels considering all possible chemical kinetics.

The stimulated emission is possible only when the population inversion condition is achieved and its probability is determined by the stimulated emission cross section (σ_{ul}), which is estimated using the relation [10],

$$\sigma_{\text{ul}}(\upsilon) = \frac{A_{\text{ul}}\lambda^2}{8\pi n^2}\,g(\upsilon)\,. \quad (8)$$

Here A_{ul} is the Einstein coefficient for the spontaneous emission characterized by the upper level radiative lifetime (τ_{r}), n is the refractive index of the medium at the emission wavelength λ and $g(\upsilon)$ is the normalized spectral line shape function at the emission frequency, ν. Considering that the medium operates at cryo-temperatures, the thermal and Doppler broadening will not be significant. Hence it is logical to use the line shape of the pump beam for present estimation of σ_{ul}. Therefore, the normalized Gaussian line shape function is considered for this estimation [10],

$$g(\upsilon) = \frac{2}{\Delta\upsilon}\left(\frac{\ln 2}{\pi}\right)^{\frac{1}{2}}\,, \quad (9)$$

where the line width $\Delta\nu$ can be written as $(c/\lambda_0^2)\,\Delta\lambda$ and hence (9) can be modified as

$$\sigma_{\text{ul}}(\upsilon) = \frac{\lambda^3}{4c\pi n^2}\,\frac{\lambda}{\Delta\lambda}\,\frac{1}{\tau_{\text{r}}}\left(\frac{\ln 2}{\pi}\right)^{\frac{1}{2}}\,. \quad (10)$$

The experimentally verified refractive index of the liquid oxygen for the visible region (4416A to 6705A) varies from 1.225 to 1.221, and for infinite wavelength it is estimated to be 1.22 [11]. The collision-induced line widths for the absorption and emission bands in oxygen have been discussed in detail in [12]. The line width is nearly 200 cm^{-1} for most pumping options and by considering a radiative lifetime of 4 s, the stimulated emission cross section for the laser emission at 1580 nm (6329 cm^{-1}) is calculated to be 2.7×10^{-23} cm^2.

Once the population inversion condition is achieved, the available (stored) laser power within the medium will be proportional to the small signal gain (γ) and the saturation intensity (I_{sat}) of the medium and is expressed as

$$P_{av} = I_{\text{sat}}\gamma LA\,. \quad (11)$$

The small signal gain and saturation intensities can be estimated using the relations

$$\gamma(\upsilon) = \sigma_{\text{ul}}(\upsilon)\left[N_\Delta - \left(\frac{g_{\text{l}}}{g_{\text{u}}}\right)N_{\text{vib}}\right]\,, \quad (12)$$

$$I_{\text{sat}} = \frac{h\upsilon}{\sigma\tau\left(1+\frac{g_{\text{l}}}{g_{\text{u}}}\right)}\,, \quad (13)$$

where N_Δ, N_{vib} are the population in the upper and lower lasing level i.e., $[O_2(^1\Delta_g)_{v=0}]$ and $[O_2(^3\Sigma_g)_{v=1}]$, respectively, τ_{u} is the lifetime of the upper level, g_{u} and g_{l} are their corresponding degeneracies. For most lasing mediums, the ratio of the degeneracies varies from 0.5 to 1, and here we considered the worst scenario, which gives a slight underestimation. Therefore, the small signal gain and saturation intensity can be rewritten as

$$\gamma(\upsilon) = \sigma_{\text{ul}}(\upsilon)\left[N_\Delta - \left(\frac{g_{\text{l}}}{g_{\text{u}}}\right)N_{\text{vib}}\right] \approx \sigma_{\text{ul}}(\upsilon)[N_\Delta - N_{\text{vib}}]\,, \quad (14)$$

$$I_{\text{sat}} = \frac{h\upsilon}{\sigma\tau_{\text{u}}\left(1+\frac{g_{\text{l}}}{g_{\text{u}}}\right)} \approx \frac{h\upsilon}{2\sigma\tau_{\text{u}}}\,. \quad (15)$$

Based on this, the gain throughout this study is simply calculated from the product of the difference in population densities between the lasing levels ($\text{d}N$) with the stimulated emission cross-section 2.7×10^{-23}. The saturation intensity for the medium is estimated to be 53 MW/cm^2, which is almost 20 times less than that of its breakdown intensity. The very low stimulated emission cross-section urges for very high pumping requirements, at the same time the high saturation intensity also yields the possibility of efficient power extraction from the medium.

3 Numerical modeling-methodology

The detailed numerical studies have been carried out to determine the temporal behavior of population in upper and lower lasing levels by considering all major source and decay mechanisms corresponding to each level. The governing rate equation for the population in upper and lower lasing

levels are expressed as follows:

$$\frac{\mathrm{d}N_\mathrm{u}}{\mathrm{d}t} = \Gamma - k_1 N_\mathrm{u} - k_2 N_\mathrm{u}^2 - \gamma N_\mathrm{u}\,, \tag{16}$$

$$\frac{\mathrm{d}N_\mathrm{l}}{\mathrm{d}t} = \Gamma + \frac{5}{4}k_1 N_\mathrm{u} + \gamma N_\mathrm{u} - k_3 N_\mathrm{l}\,, \tag{17}$$

where N_u and N_l are the population of the upper $O_2(^1\Delta_g)_{v=0}$ molecules and lower $O_2(^3\Sigma_g)_{v=1}$ molecules, respectively, and k is the rate constant for the various probable decay or quenching processes in liquid oxygen:

$$\mathrm{O_2}(^1\Delta_g)_{v=0} + \mathrm{O_2}(^3\Sigma_g)_{v=0} \rightarrow 2\mathrm{O_2}(^3\Sigma_g)_{v=0}\,,$$
$$k_1 = 1.05\times10^{-18}\,\mathrm{cm^3 mol^{-1} s^{-1}}\,, \tag{18}$$
$$\mathrm{O_2}(^1\Delta_g)_{v=0} + \mathrm{O_2}(^1\Delta_g)_{v=0} \rightarrow 2\mathrm{O_2}(^3\Sigma_g)_{v=0} + 635\,\mathrm{nm}\,,$$
$$k_2 = 1.7\times10^{-18}\left(\frac{T_0}{T}\right)^{-\frac{1}{2}}\,\mathrm{cm^3 mol^{-1} s^{-1}}\,, \tag{19}$$
$$\mathrm{O_2}(^1\Delta_g)_{v=0} \rightarrow \mathrm{O_2}(^3\Sigma_g)_{v=1} + 1580\,\mathrm{nm}\,,$$
$$\gamma = \frac{1}{4}\,\mathrm{s^{-1}}\,, \tag{20}$$
$$\mathrm{O_2}(^1\Delta_g)_{v=0} + 4\mathrm{O_2}(^3\Sigma_g)_{v=0} \rightarrow 5\mathrm{O_2}(^3\Sigma_g)_{v=1} + \Delta E = 106\,\mathrm{cm^{-1}}\,,$$
$$k = \frac{5}{4}k_1,: \quad \text{where} \quad -k_1 = 1.05\times10^{-18}\,\mathrm{cm^3 mol^{-1} s^{-1}}\,, \tag{21}$$
$$\mathrm{O_2}(^3\Sigma_g)_{v=1} + \mathrm{O_2}(^3\Sigma_g)_{v=0} \rightarrow 2\mathrm{O_2}(^3\Sigma_g)_{v=0}\,,$$
$$k_{vT} = k_3 = 400\,\mathrm{s^{-1}}\,. \tag{22}$$

The pump rate, Γ is governed by the following equation,

$$\Gamma = n\alpha\frac{P_\mathrm{l}}{A(h\upsilon)}\,, \tag{23}$$

where P_l is the incident pump power, 'A' is the focused beam area, 'α' absorption coefficient ($\mathrm{cm^{-1}}$) corresponding to the pump wavelength, 'n' is the number of ground state molecules pumped by each incident photon ($n = 1$ for 1064 nm, $n = 2$ for 634 nm) to the singlet delta state, '$h\upsilon$' is the incident single photon energy. The same relation is utilized for determining the rate of pumping to the first vibrational state as well, but is zero for the case of pumping wavelength being 634 nm and is a non-zero quantity for 1064 nm.

Equations (16) and (17) are solved using finite difference method in an explicit formulation. The finite difference method is distinctly better as compared to the analytical approach for the present system. The reason being that the numerical solution requires solving simple algebraic functions as compared to solution of highly computationally intensive exponential and logarithmic functions in analytical approach. Another reason for preferring the former approach is the easier prediction of variation in number densities at various locations along and normal to the cell for a host of pumping possibilities. Figure 3 shows a typical case of the liquid oxygen cell, irradiated with a Gaussian pumping beam, discretized into a grid of 11×5. The numerical code employed has provisions for using wide ranges of gird arrays along with the possibility of employing non-uniform grids. This would allow packing of more number of grids in the region of larger gradients. Since the beam profile and the cell are symmetric with respect to the x-axis, the behavior of grids lying on the one side of the axis of symmetry will be identical with that on the other. Thus, only one half of the cell is considered for modeling to reduce the computational effort.

In finite difference form, the rate equations (16) and (17) can be expressed as

$$N_\mathrm{u}(t+\Delta t) = \Gamma\Delta t - k_1 N_\mathrm{u}(t)\Delta t - k_2 N_\mathrm{u}(t)^2\Delta t - \gamma N_\mathrm{u}(t)\Delta t\,, \tag{24}$$

$$N_\mathrm{l}(t+\Delta t) = \Gamma\Delta t + \left(\frac{5}{4}\right)k_1 N_\mathrm{u}(t)\Delta t + \gamma N_\mathrm{u}(t)\Delta t - k_3 N_\mathrm{l}(t)\Delta t\,. \tag{25}$$

For all cases in this study, the time step (Δt) for the solution of the above equations is considered to be lower than the time associated with the fastest occurring physical process. For example, in case of continuous pumping the fastest occurring process is the decay of the upper lasing level, which is of the order of several tens of microseconds. Thus, in continuous pumping case the assumed time step is in between 1–10 μs. At the same time, for the pulsed pumping case the fastest phenomenon is the pumping process itself and hence the time step duration is taken to be smaller than the pump laser pulse duration. The results presented in this paper have also been checked for independency of time steps. Furthermore, in order to assess the cumulative response of the entire medium in the liquid cell, the representative densities of both levels at any given moment are obtained by spatially averaging the same over the generated grid. The relations employed

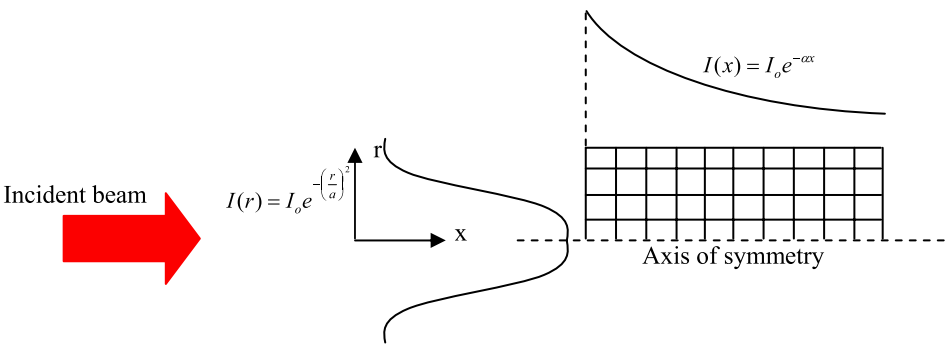

FIGURE 3 Grid geometry of optical pumping used for numerical modeling

for spatial averaging are given below,

$$N_{\mathrm{um}}(t) = \frac{\sum N_{u_{i,j}}(t)}{i \times j}, \tag{26}$$

$$N_{\mathrm{lm}}(t) = \frac{\sum N_{l_{i,j}}(t)}{i \times j}, \tag{27}$$

where 'i' and 'j' are the number of grid points in the 'x' and 'r' direction, respectively. Thus, the developed code not only predicts the response to the input pumping power at various locations along and across the cell but also predicts the average response of the medium. It can be utilized for subsequent estimation of the range of expected gain and the corresponding extractable power output.

4 Results and discussions

For pure natural liquid oxygen, the upper laser level has a non-radiative lifetime (τ_{u}) of about 44 μs, while the lower level (τ_{l}) has relatively longer non-radiative lifetime of about 2.5 ms [13]. This property of pure natural liquid oxygen makes pumping very critical which is associated with accumulation of population at the lower laser level. The rate of accumulation will determine the limit of population inversion duration and hence the small signal gain in this medium. This means, for a continuous population inversion and gain, that it is essential to either increase τ_{u} or decrease τ_{l} or simultaneously do both by some means. Experiments have also proven that the lifetime of the singlet delta oxygen is more in case of isotopic liquid oxygen medium as compared to that in pure natural liquid oxygen [14] medium. On the other hand there is experimental evidence that some impurity addition can play a role in the VT relaxation rate of the lower level [8]. By considering these aspects, three different oxygen-rich mediums in liquid phase viz: (i) natural liquid oxygen (ii) isotopic liquid oxygen and (iii) liquid air are considered in this study. We have numerically analyzed the evolution of population in both lasing levels and verified the possible population inversion duration under different pumping conditions viz. wavelength and pump intensities.

Two different wavelength sources at 634 nm and 1064 nm are considered for the analysis. Liquid oxygen has high absorption coefficients for the above wavelengths, and hence it is not useful to have a gain length longer than 1 or 2 cm along the pump direction. Therefore, in the present study, a liquid cell of 1 cm length has been taken with the consideration that pumping beam of different power levels is focused to a fixed diameter. For the studies presented here, the beam energy is considered to be focused to 3 mm diameter and is passed only once through the length of the liquid cell. Simulations are carried out for various energies of the pump lasers to have various power densities and hence pump rates. The rate constants for various processes used in this simulation studies are mostly experimentally accepted ones, making the simulation results reliable. The time evolution of the population at the upper and lower levels obtained from (24) and (25) is averaged over the illuminated volume [(26) and (27)] and utilized to calculate the corresponding gain profile employing equation (14). The results obtained in each case are discussed below.

4.1 *Natural liquid oxygen*

In pure natural liquid oxygen, there are various reported values for singlet oxygen quenching with ground state molecules (k_1) and its self-pooling rate (k_2). The reported values of self-pooling rate of singlet oxygen in liquid oxygen have wide conflicts. The earlier work by H. Klingshern et al. [14] had reported a value of $3 \pm 1 \times 10^{-15}\,\mathrm{cm^3/mol/s}$, while the recent experiments by K.R. Hobbs et al. [15] reported a value of $1 \pm 0.5 \times 10^{-17}\,\mathrm{cm^3/mol/s}$, which was almost a two-order difference. While the variation in quenching rates are minimal, we have considered the most accepted value of $2.2 \times 10^4\,\mathrm{s^{-1}}$, which is experimentally proved from the fluorescence decay signal [14]. The most accepted decay rate of the lower lasing level (k_3), estimated theoretically and observed experimentally, is $400\,\mathrm{s^{-1}}$ [7]. Therefore, the rate constants used for the simulation of natural liquid oxygen are $k_1 = 2.2 \times 10^4\,\mathrm{s^{-1}}$, $k_2 = 1.0 \times 10^{-17}\,\mathrm{cm^3/mol/s}$, $k_3 = 400\,\mathrm{s^{-1}}$ and $\gamma = 0.25\,\mathrm{s^{-1}}$.

The simulation results for continuous wave (cw) pumping of natural liquid oxygen with 634 nm wavelength source for three different power levels of 1 W, 1 kW and 1 MWare presented in Fig. 4a–c, respectively. The pumping of the same medium with 1064 nm source having 1 kW power is shown in Fig. 4d. The validation of the results is carried out by comparing the singlet delta population in our estimations with the same obtained by the recently reported modeling results of K.R. Hobbs et al. [15], which they have also verified experimentally. From Fig. 4b and d, it is clear that the gain in case of 634 nm source pumping is almost 35% more compared to that with 1064 nm source. It is clear that a positive gain is obtained in this medium for about 65 μs and 57 μs for 634 nm and 1064 nm sources, respectively, is almost independent of the pump power. The singlet delta concentration and small signal gains are found to be almost linear with the pump power, which shows the possibility of near linear power scale up of the laser with the pump power. The deviations at very high pump intensities ($\sim \mathrm{MW/cm^2}$) are due to the dominance of pooling process at large singlet oxygen densities showing that efficient utilization of the medium needs optimized pump intensity.

The results for pumping of natural liquid oxygen with 10 ns pulsed laser at 1064 nm wavelength for two different energies of 1 J and 10 J are given in Fig. 5a and b, respectively. It is evident from the results that in case of pulsed pumping, obtained peak gain is linearly proportional to the pump energy for the reason that the decay processes are not able respond with in this time scale. The population inversion duration is found to be much larger than the pump pulse duration and hence natural liquid oxygen is a potential medium for pulsed lasers. The small signal gain obtained with 1 MW power cw pumping ($0.02\,\mathrm{cm^{-1}}$) and 10 J, 10 ns pulsed pumping ($0.01\,\mathrm{cm^{-1}}$) looks reasonable for obtaining lasing with better extraction efficiencies, provided the cavity losses can be minimized to less than 0.5%. These issues are addressed in forthcoming section on power extraction. It means that the medium can be utilized for lasing, if it can be pumped

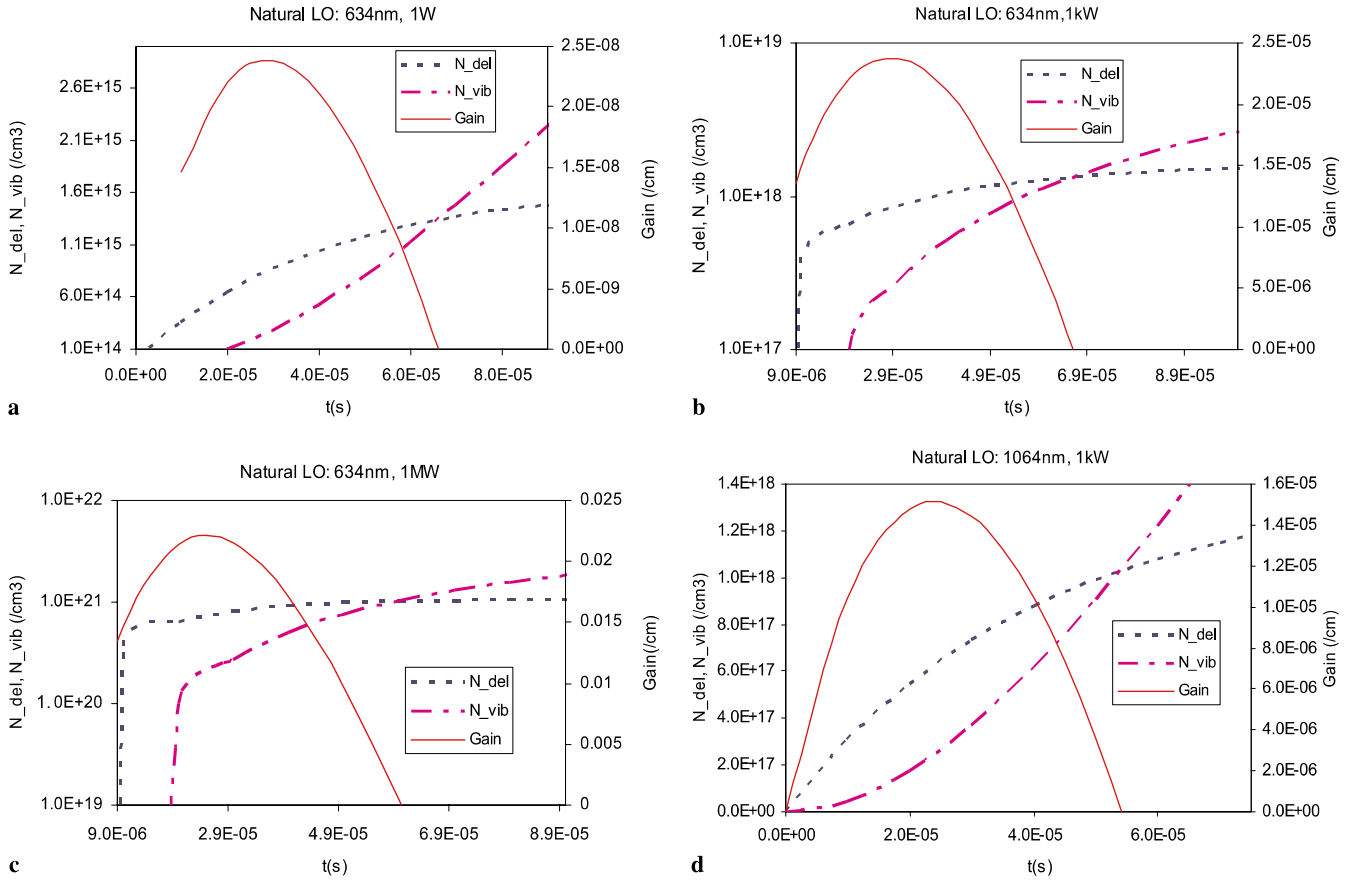

FIGURE 4 (**a**) The populations of the upper and lower lasing levels and the small signal gain for pumping with 634 nm source with 1 W power; (**b**) The populations of the upper and lower lasing levels and the small signal gain for pumping with 634 nm source with 1 kW power; (**c**) The populations of the upper and lower lasing levels and the small signal gain for pumping with 634 nm source with 1 MW power; (**d**) The populations of the upper and lower lasing levels and the small signal gain for pumping with 1064 nm source with 1 kW power

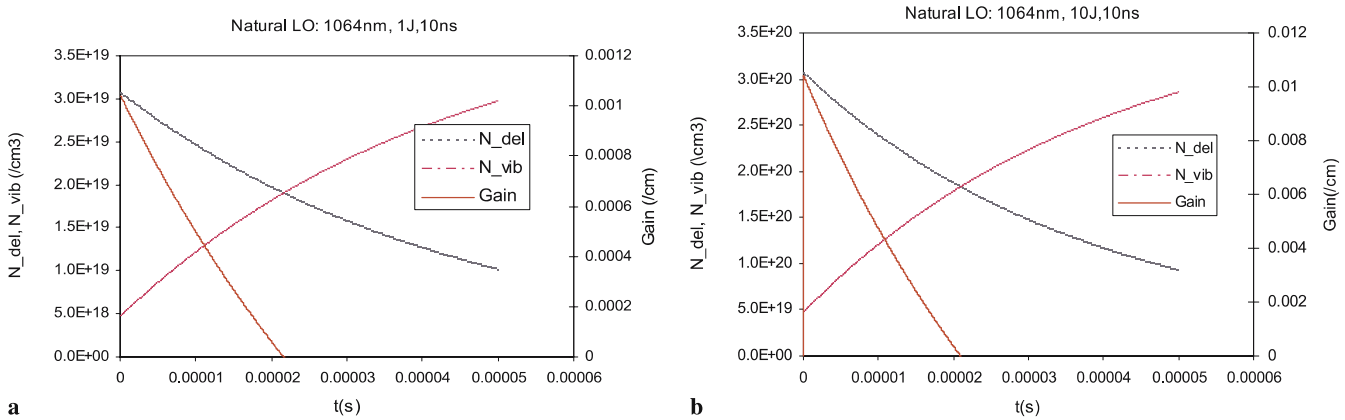

FIGURE 5 (**a**) The populations of the upper and lower lasing levels and the small signal gain for pumping with 1064 nm source with $E = 1.0$ J and 10 ns duration; (**b**) The populations of the upper and lower lasing levels and the small signal gain for pumping with 1064 nm source with $E = 10.0$ J and 10 ns duration

with intensities of the order of few MW/cm^2. But the only concern with natural liquid oxygen is the time duration of positive gain, which limits its use as a possible cw lasing medium.

4.2 *Isotopic liquid oxygen*

The lifetime, τ_u, of $O_2(^1\Delta_g)_{v=0}$ is experimentally found to be improved in isotopic liquid oxygen ($^{18}O_2$) from 44 µs to about 10 ms [14]. The quenching of $O_2(^1\Delta_g)_{v=0}$ molecules with the ground state molecules $O_2(^3\Sigma_g)_{v=0}$ has a drastic isotopic effect, making k_1 considerably smaller in isotopic liquid oxygen $^{18}O_2$ than for natural liquid oxygen $^{16}O_2$. The reasons for this are detailed in [13]. The above work also reports that the V–T relaxation rate for the first vibrational level of ground molecules in isotopic liquid oxygen is still 400 s^{-1}, which is the same as that for natural liquid oxygen. At the same time, H. Klingshirn et.al have reported that

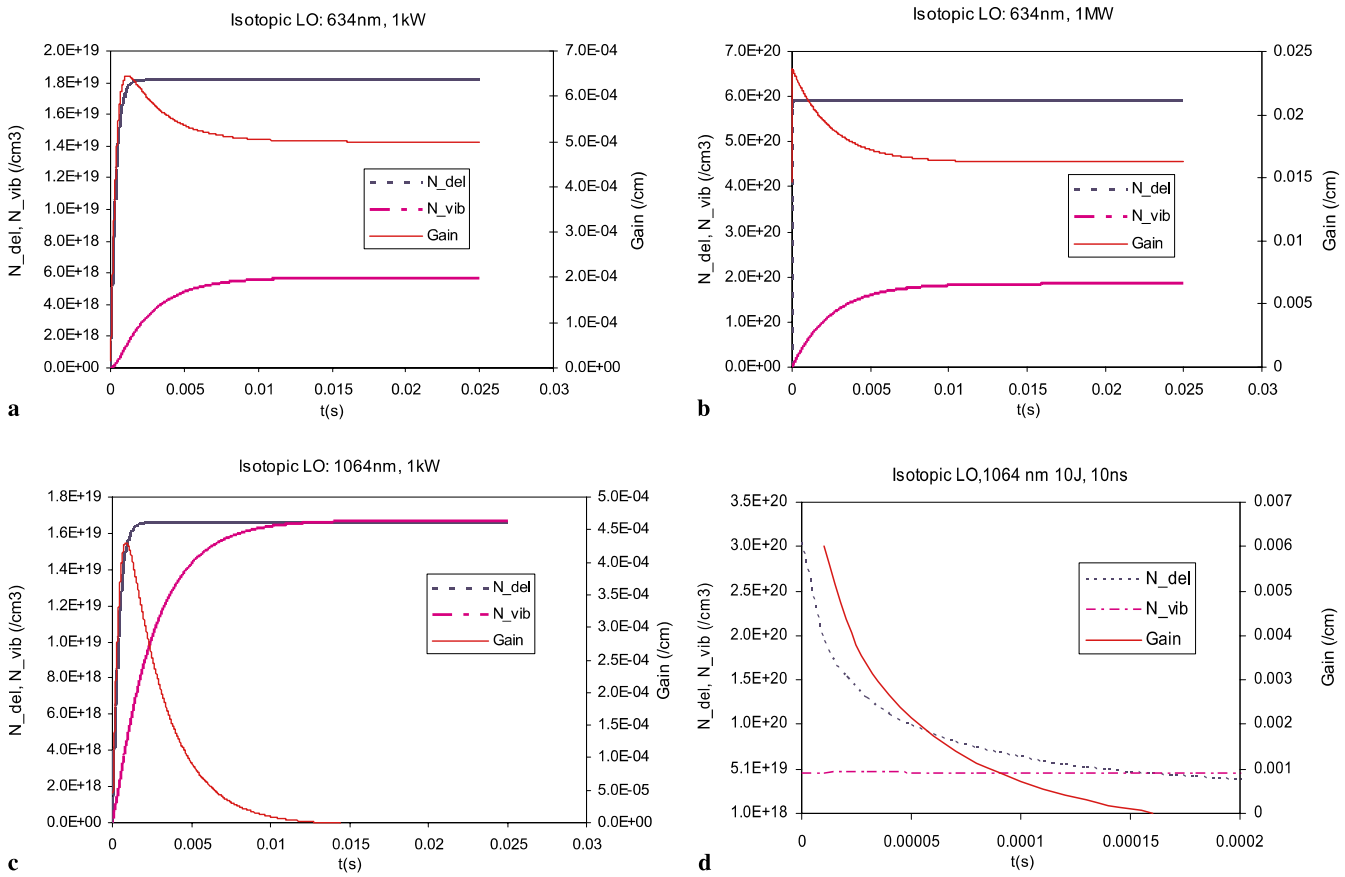

FIGURE 6 (**a**) The populations of the upper and lower lasing levels and the small signal gain for cw pumping with 634 nm source with 1 kW power; (**b**) the populations of the upper and lower lasing levels and the small signal gain for cw pumping with 634 nm source with 1 MW power; (**c**) The populations of the upper and lower lasing levels and the small signal gain for cw pumping with 1064 nm source with 1 kW power; (**d**) The populations of the upper and lower lasing levels and the small signal gain for pulsed pumping with 1064 nm source 10 J, 10 ns pulse

the pooling rate of $O_2(^1\Delta_g)_{v=0}$ molecules in isotopic liquid oxygen is an order of magnitude higher than in natural liquid oxygen [14].

Based on the above discussions, the rate constants considered for the analysis on isotopic liquid oxygen are the following: $k_1 = 100\,s^{-1}$, $k_2 = 1.0 \times 10^{-16}\,cm^3/mol/s$, $k_3 = 400\,s^{-1}$ and $\gamma = 0.25\,s^{-1}$. The simulation results for continuous wave pumping with 634 nm wavelength source for two different power levels of 1 kW and 1 MW are shown in Fig. 6a and b, while the results for pumping with 1064 nm source for 1 kW cw power and 10 J, 10 ns pulse are given in Fig. 6c and d respectively. The results indicate that pumping with 634 nm source yields a continuous population inversion for very large duration. At the same time while pumping with 1064 nm source, the population inversion duration is reduced to only 10 ms, which is still larger compared to that of natural liquid oxygen. However, as in the case of natural liquid oxygen, the population inversion duration is found to be independent of the pumping power. Further, for low pump power (for example the case of 1 kW), it is found that the small signal gain in isotopic liquid oxygen is large as compared to that in natural liquid oxygen. However, the small signal gain is almost the same for the case of high pump power ($\sim$ 1 MW). The reason for this result is that at very high pumping intensities, pooling becomes the dominant loss mechanism compared to that of quenching, which will balance the population in both levels much faster.

4.3 *Liquid air*

In case of natural liquid oxygen and isotopic liquid oxygen discussed earlier, the lower level lifetime remains the same, while the upper level lifetime is found to improve for the latter. In these studies, the lifetime of the lower lasing level mainly depends on the vibrational to translational conversion (V–T) and is about 2.5 ms. But there is clear evidence from the experiments that the V–T relaxation rate constants are highly dependent on the impurities (like Ar, Kr, Xe, CO_2, H_2O etc.) present in the liquid oxygen, and experimentally it was observed to be $\sim$ 50 μs by Renner et al. [8]. This drastic reduction of the lower level lifetime by the impurities may be explored and gives hope for a reasonably long continuous population inversion condition in impure liquid oxygen. The influence of the impurities on the lifetime of the $(^1\Delta_g)_{v=0}$ molecules has not been reported by any one to the best of our knowledge. Furthermore, it is also interesting to note that the quenching rate of the upper level is found to reduce almost linearly with the percentage of oxygen present in the mixture along with buffer medium such as O_2/N_2 or O_2/Ar etc., which improves the lifetime τ_u [2] as well. However, it should also be remembered that the absorption coefficient for the pump beam

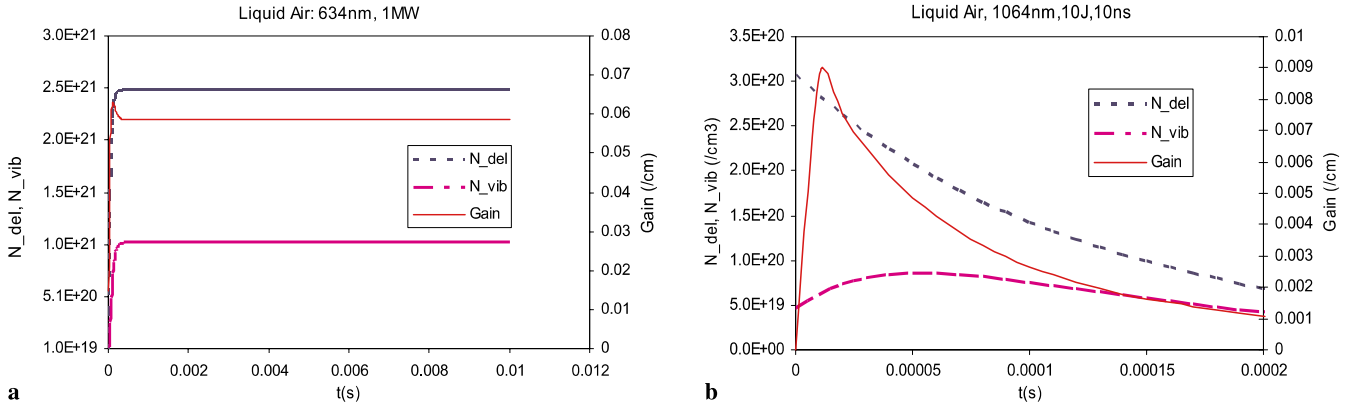

FIGURE 7 (**a**) The populations of the upper and lower lasing levels and the small signal gain for cw pumping of liquid air medium with 634 nm source having 1 MW power; (**b**) The populations of the upper and lower lasing levels and the small signal gain for pulsed pumping of liquid air medium with 1064 nm having 10 J, 10 ns

will be reduced with oxygen density reduction [5], which may require multiple passage of the beam for efficient pumping.

In order to explore this idea, liquid air, where there is availability of almost 21%–22% of liquid oxygen and rest liquid nitrogen has been considered for the analysis. Here we have assumed that the liquid air has sufficient impurities to reduce the lifetime of the lower vibrational levels to about 50 μs. Since nitrogen is a buffer medium, it typically does not affect the lifetime of electronic energy levels. The reduction in the quenching and pooling rates is proportional to the oxygen density in liquid air, which is less as compared to that in pure liquid oxygen. Therefore, for the analysis of liquid air, we have considered rate constants as the follwoing: $k_1 = 4.4 \times 10^3\ \mathrm{s}^{-1}$, $k_2 = 2 \times 10^{-18}\ \mathrm{cm}^3/\mathrm{mol/s}$, $k_3 = 20\,000\ \mathrm{s}^{-1}$ and $\gamma = 0.25\ \mathrm{s}^{-1}$. The studies are carried out for both cw and pulsed pumping for various intensities at 634 nm and 1064 nm. However, the simulation results for the case of continuous wave (cw) pumping with 1 MW source at 634 nm and the same for pulsed pumping with 10 J, 10 ns pulse at 1064 nm are only presented here in Fig. 7a and b respectively.

In case of pumping with a continuous source, it is found that a stable gain and continuous population inversion condition occurs while pumping with either of the wavelength sources unlike in other two discussed mediums. The gain obtained in liquid air at lower pumping power (say 1 kW or less) is relatively less compared to both natural and isotopic liquid oxygen due to the reduction in the excitation rate because of the low oxygen density available. But for very high pump power (∼ 1 MW), the gain obtained with liquid air medium is much higher compared to both natural as well as isotopic liquid oxygen. This clearly indicates the role of self pooling at high density production of upper lasing level molecules in mediums characterized with high oxygen density (natural, isotopic oxygen). In case of pulsed pumping with nanosecond pulses, the gain is almost linear with the pump energy and nearly the same for all the three mediums.

5 Output power estimation

The extractable output power from the lasing medium is proportional to the available power in the medium and is expressed as:

$$P_{\mathrm{ext}} = P_{av}\eta_{\mathrm{ext}}\,, \tag{28}$$

where η_{ext} is the extraction efficiency expressed by the product of the medium extraction efficiency (η_{extm}) and the resonator extraction efficiency (η_{extr}). The medium and resonator extraction efficiency can be estimated using the following set of Rigrod relations [16] as

$$\eta_{\mathrm{extm}} = 1 - \left(\frac{\gamma_{\mathrm{th}}}{\gamma_0}\right)\,, \tag{29}$$

$$\eta_{\mathrm{extr}} = \frac{t}{t+a} = \frac{\gamma_{\mathrm{th}}(2L) - a}{\gamma_{\mathrm{th}}(2L)}\,, \tag{30}$$

where the threshold gain (γ_{th}) essential for lasing is dependent on the gain length L, resonator coupler mirror transmission (t) and the absorption loss (a) of the resonator mirrors, which can be expressed as

$$\gamma_{\mathrm{th}} = \frac{t+a}{2L}\,. \tag{31}$$

For mediums having very low stimulated emission cross-section, very large pumping power is essential to obtain the threshold gain to overcome the resonator losses. In such mediums, typically, the available gain will be near to the threshold gain and hence the medium extraction efficiency will be very low. However, if the medium has high saturation intensity, it can have high amplification through proper selection of the resonator mirrors and can yield high output power. The calculation shows that the extraction efficiency for this medium is highly dependent on the small signal gain. Hence, for a high gain case of 0.06 cm^{-1}, an extraction efficiency of about 60% can easily be obtained provided the resonator loss is limited to less than 0.5%. The extractable energy in case of pulsed pumping and possible output power in case of continuous pumping are estimated employing the relations [10],

$$E_{\mathrm{out}} = E_{\mathrm{sat}}AT(1-a)\left[\frac{-2\gamma_0 L}{\ln(1-\alpha-T)} - 1\right]\,, \tag{32}$$

$$P_{\mathrm{out}} = I_{\mathrm{sat}}AT(1-a)\left[\frac{-2\gamma_0 L}{\ln(1-\alpha-T)} - 1\right]\,, \tag{33}$$

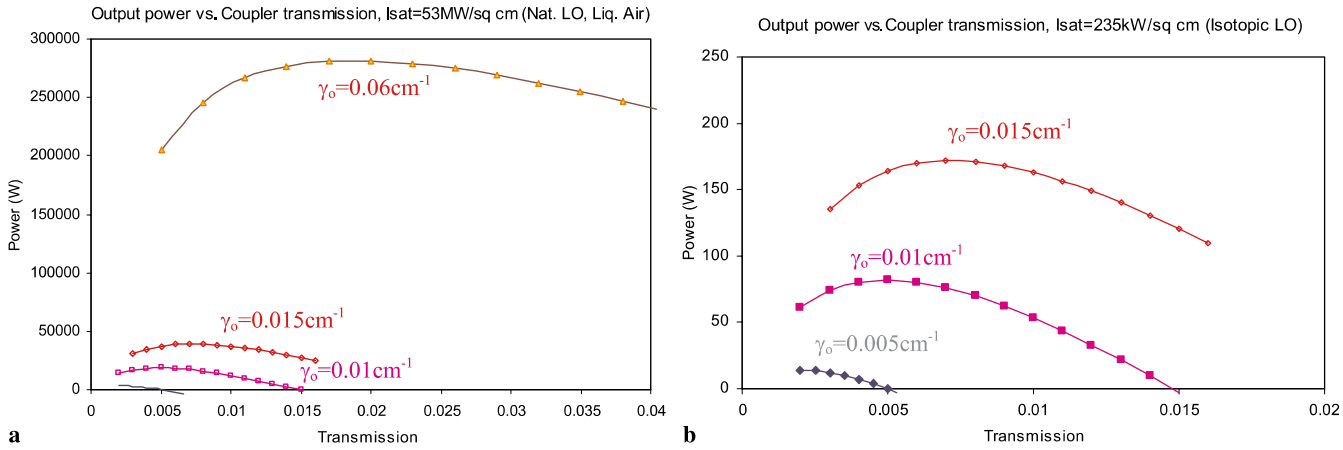

FIGURE 8 (**a**) The output power with coupler transmission for natural liquid oxygen and liquid air under different gain conditions and continuous pumping; (**b**) Change in output power with coupler transmission for isotopic liquid oxygen under different gain conditions during continuous pumping

where E_{sat}, A are the saturation energy density, area of cross-section of the gain medium respectively and α is the absorption loss in the medium. The saturation intensity for natural liquid oxygen and liquid air are considered to be the same due to their identical upper level lifetime. But the saturation intensity for the isotopic liquid oxygen will be much less because of its relatively large lifetime and is estimated to be $\sim 230\,\mathrm{kW/cm^2}$.

In case of continuous pumping, the estimated output power for the gain values predicted by modeling ranging from $0.005\,\mathrm{cm^{-1}}$ to $0.06\,\mathrm{cm^{-1}}$ corresponding to natural liquid oxygen and liquid air are plotted in Fig. 8a and the same for isotopic liquid oxygen is shown in Fig. 8b. For the observed gain of $0.06\,\mathrm{cm^{-1}}$ for 1 MW pumping in liquid air, the analysis predicts a photon conversion efficiency of more than 25%. At the same time, for pure natural liquid oxygen it is only less than 5% due to the smaller gain obtained in the medium for the same pump power. Further, the photon conversion efficiency is found to be too low in isotopic liquid oxygen, i.e., only 0.02% compared to 4.5% in liquid air for the same gain value of $0.015\,\mathrm{cm^{-1}}$ for the reason that it has very low saturation intensity. Typically, the small signal gain is found to be a function of the pump wavelength. Thus, the gain obtained is almost 35% more in case of 634 nm pumping as compared to that of 1064 nm pumping, the corresponding photon conversion efficiency is also found to be proportionally higher.

In case of pulsed pumping, the energy output is almost the same for all mediums and dependent only on the gain since E_{sat} is dependent only on the stimulated emission cross-section. The predicted energy output variation with a coupler transmission for different gain values is shown in Fig. 9. The results indicate that an energy conversion efficiency of about 16% is possible with these mediums.

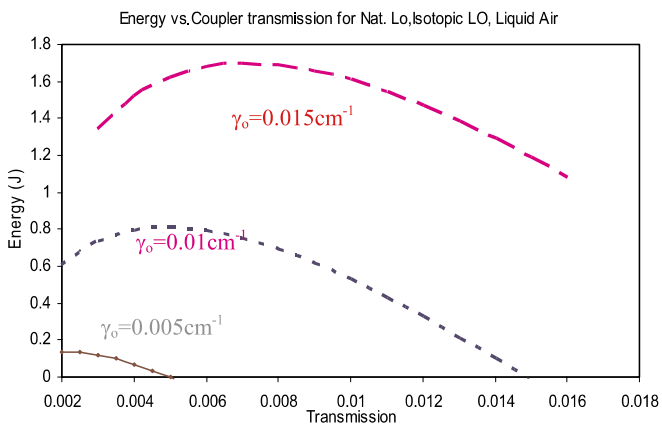

FIGURE 9 Change in output energy with coupler transmission for natural, isotopic liquid oxygen and liquid air under different gain conditions and pulsed pumping

6 Realization criticalities

Major practical challenges in the realization of liquid oxygen laser have been addressed along with certain solutions in [17]. Apart from these, one such criticality anticipated is the thermal distortions of the beams due to the heating of the lasing medium. This occurs due to the chemical kinetics of the molecules in the medium during the excitation process. The V–T relaxation process (22) is the one, which results in slow heating of the solution with energy release of about 0.19 eV in each transition. We have estimated the temperature rise by incorporating this energy release with the corresponding decay rate and found that nearly 1%–3% of the pump energy is dumped resulting in heating of the medium for pump power of 1 MW to 1 kW. At high pump power the fraction is less because the pooling process dominates the other decay processes viz, V–V and V–T relaxations. In the case of pulsed pumping with low repetition rate, it is found that the liquid medium will not undergo any physical change due to the small amount of energy dumped during the pump duration. In case of very high power (1 MW) cw pumping, it is found that the heat dumping can affect the physical stability since the heat dump rate is more than the latent heat of vaporization ($2934\,\mathrm{BTUlb^{-1}mol^{-1}}$) of the liquid. In such cases, it will be essential to use either super-cooled liquid with cooling provisions to maintain its temperature or to use replenishing lasing medium to avoid the temperature rise of the medium.

The temperature rise of the medium can also cause a refractive index profile within the medium and may induce thermal blooming effects and distortion of the beam. Experimental studies on such thermal blooming effects and beam

distortions in liquid nitrogen are discussed in [18]. In case of pulsed pumping with less repetitive pulses the natural convection will take care of the thermal effects hence reducing beam distortions. But in case of steady state cw pumping or high repetitive pulsed pumping, these distortions will be transient for initial pump duration and will reach an equilibrium condition for the remaining duration. In the present studies we have considered the cases where around 80% (wavelength dependent) of the beam is absorbed within the medium and estimated the average populations of the various levels and hence will not affect the computed results.

7 Conclusion

The present studies indicate that oxygen rich cryosolutions can be an effective lasing medium with excellent photon conversion efficiency. The results indicate that reasonable small signal gain for lasing action is achievable only when pump intensity is close to MW/cm^2. The simulations indicate that in all the three mediums considered here, pumping with 634 nm source gives higher small signal gain in both continuous and pulsed mode as compared to that with 1064 nm source. The analysis shows that liquid air medium is highly potential for continuous wave lasers when pumping with either 1064 nm or 634 nm source while isotopic liquid oxygen is suitable only when pumping with 634 nm source. It is also found that pure natural liquid oxygen is a suitable medium only for pulsed lasers and continuous gain is available only for few milliseconds. Liquid air shows reasonable small signal gain, and for a case of MW level pumping, it is about $0.06\,cm^{-1}$ with a corresponding photon conversion efficiency of about 25%. Although, isotopic liquid oxygen is suitable for continuous wave lasing, it provides a low photon conversion efficiency because of the low saturation intensity of the medium. Also, for very large pump intensity, pooling loss is the dominant process governing the small signal gain. Hence, liquid air is the most potential medium, since it is associated with lower pooling losses due to the presence of buffer nitrogen. We are in progress of setting up the experimental setup for the studies with these mediums, which will surely shed more light on this possible lasing medium.

REFERENCES

1 R.K. Tyagi, R. Rajesh, G. Singhal, Mainuddin, A.L. Dawar, M. Endo, Opt. Laser Technol. **35**, 395 (2003)
2 D.L. Huestis, G. Black, S.A. Edelstein, R.L. Sharpless, J. Chem. Phys. **60**, 4471 (1974)
3 www.newscientisttech.com or New Scientist Magazine, Issue 2514, 25th August 2005, p. 24
4 B.V. Zhadanov, K.R. Hobbs, T.L. Henshaw, D.K. Neumann, SPIE **5334**, 70 (2004)
5 A. Yamagishi, T. Ohta, J. Konno, H. Inaba, J. Opt. Soc. Am. **71**, 1197 (1981)
6 R. Protz, M. Maier, J. Chem. Phys. **73**, 5464 (1980)
7 R. Protz, M. Maier, Chem. Phys. Lett. **64**, 2731 (1979)
8 G. Renner, M. Maier, Chem. Phys. Lett. **28**, 614 (1974)
9 A.R.W. McKellar, N.H. Rich, H.L. Welsh, Canad. J. Phys. **50**, 1 (1972)
10 W. Koechner, *Solid State Laser Engineering*, 5th revised edn. (Springer, Berlin, 1999)
11 J.A. Fleming, J. Dewar, Proc. Royal Soc. London **60**, 358 (1896–1897)
12 R. Roger, P. Blickensderfer, G.E. Ewing, J. Chem. Phys. **51**, 5284 (1968)
13 E. Wild, H. Klingshirn, B. Faltermeir, M. Maier, Chem. Phys. Lett. **93**, 490 (1982)
14 H. Klingshirn, B. Faltermeier, W. Hengl, M. Maier, Chem. Phys. Lett. **93**, 485 (1982)
15 R. Hobbs, B.V. Zhdanov, T.L. Henshaw, D.K. Neumann, SPIE **5334**, 100 (2000)
16 W.W. Rigrods, J. Appl. Phys. **14**, 2602 (1963)
17 D.L. Huestis, Chem. Phys. Lett. **411**, 108 (2005)
18 E. Wild, M. Maier, J. Appl. Phys. **51**, 3078 (1980)